Spokesman Uriel Nauenberg
Tel (303) 492-7715
-7901
-8713

A Measurement of the Longitudinal Polarization of Lambdas at Large Transverse Momenta in the Reaction $p + N \rightarrow \Lambda + X$

David Bartlett, David McQuate, Robert Morse,
Marshall Mugge, Uriel Nauenberg
University of Colorado
Boulder, Colorado 80302

Table of Contents

		Page
1)	Abstract	3
2)	Introduction	4
3)	Theoretical Expectations	5
4)	Experimental Aspects	7
	I) $\Lambda^{\circ}K^{\circ}$ separation	8
	II) General Particle Background	9
	III) The Need for Cerenkov Counters	11
	IV) Systematic Experimental Biases and the Precession of the Λ° Spin	11
	V) Λ° from Ξ Decays	13
5)	The Detector	14
	A) Sweeping Magnet and Shielding	15
	B) The Neutral Channel	15
	C) The Decay Region	16
	D) The V Spectrometer	16
	E) The Proton Detector	17
	F) The Gamma Detector	18
6)	Resolution	18
7)	V Detection Efficiency	19
8)	Data Taking Plan	20
9)	Expected Λ° Rates	21
10)	Future Group Commitments	21
11)	Equipment Needs	22

12) Tables

1) Λ° Expected Rates 23

2) Detector Dimensions and Details 25

3) Cost Estimates 27

13) References 28

14) Figures 31

Abstract

We plan to measure the longitudinal (parity - violating) polarization of lambdas at large transverse momenta in the reaction $p + N \rightarrow \Lambda^{\circ} + X$. We propose doing this by measuring the angular distribution of the proton in the subsequent decay $\Lambda^{\circ} \rightarrow \pi^{-} + p$. At the same time we can measure the distribution at large transverse momentum of lambdas in the reaction $p + N \rightarrow \Lambda^{\circ} + X$ and of kaons in the reaction $p + N \rightarrow K_S^{\circ} + X$. We expect to be sensitive to transverse momenta from 2 to 6 GeV/c.

Introduction

We propose to measure the longitudinal polarization of the Λ^os by measuring the forward-backward symmetry of its decay. The presence of such a polarization is evidence for a parity violating type of process. This can occur either because of the presence of a weak interaction in the collision process or because of the weak decay of new particles being produced, like "charm" particles. We propose to measure these effects for transverse momenta between 2 and 6 Gev/c. This implies carrying out measurements down to a cross section of 10^{-37} cm^2, a region where weak interactions might manifest themselves. Simultaneously, we will measure the invariant cross section $Ed^3\sigma/d^3p$ as a function of transverse momentum for Λ^o and also K^o .

The detection of the weak interaction effects in the collision of hadrons, is an extremely interesting and challenging experimental problem that has not been attempted so far. In fact, one of the major reasons for the construction of accelerators that lead to higher center of mass energy collisions, like POPAE, ISA, PEP, is to attempt to reach an energy realm where weak interaction effects should be present.(1) Another source of weak interaction effects not observed so far could be the copious production of baryonic charm states at FNAL energies. These particles are supposed to decay weakly and a large number of Λ^os at relatively large transverse momenta should be present. These should have a longitudinal polarization typical of these weak decays; namely, of the order of 30% like

in Λ^o and Ξ decays. We propose to search for these effects at FNAL energies.

At the same time the study of the production of hadrons at large transverse momenta has been of topical interest in the last few years. It bears on the nature of interactions at small distances and the quark like structure of hadrons[2,3,4]. The production of strange baryons at large transverse momenta has not yet been studied.

Theoretical Expectations

If we assume the weak $\Delta S = 1$ hadronic weak interactions can be related to the $\Delta S = 0$ neutrino interactions by[5]

$$\sigma(\Delta S=1) = 10\sin^2\theta\ \sigma(\Delta S=0)$$
$$= 10\sin^2\theta \times 10^{-38} E_{lab}(\text{Gev})\ \text{cm}^2/\text{nucleon}$$

where θ is the Cabibbo angle then the cross section for E_{lab} = 300 Gev/c on a tungsten target becomes

$$\sigma(\Delta S=1) = .2\times10^{-38}\times300\times(184)^{2/3}$$

$$= 2\times10^{-35}\ \text{cm}^2/\text{nucleus}$$

To obtain the weak differential cross section we assume the following form for it

$$\frac{Ed^3\sigma}{d^3p} = \frac{E}{2\pi}\ \frac{1}{p_\perp}\ \frac{d\sigma}{dp_\perp}\ \frac{d\sigma}{dp_\parallel}$$

$$\frac{d\sigma}{dp_\perp} = C\ e^{-Ap_\perp}$$

$$\frac{d\sigma}{dp_\parallel} = (1 - x)^{7/2}$$

where $x = p_{\parallel}$ (c.m.)/p_{max}(c.m.) and C, A are const.

We can obtain C from the relation

$$\sigma_{weak} = \sigma = \iint \frac{d\sigma}{dp_{\perp}} \frac{d\sigma}{dp_{\parallel}} dp_{\perp} \, dp_{\parallel}$$

from which we obtain

$$C = \frac{2.2 \, \sigma A}{p^*_{max}}$$

Since we want the weak differential cross section for $x \simeq 0$ we get

$$\frac{Ed^3\sigma}{d^3p} = \frac{E}{2\pi} \frac{1}{p_{\perp}} \frac{2.2 \, \sigma A}{p^*_{max}} e^{-Ap_{\perp}}$$

and for θ = 80 mrads

$$\frac{Ed^3\sigma}{d^3p} = 8 \times 10^{-36} \, Ae^{-Ap_{\perp}}$$

Hence we can obtain a table of the cross section we get for $p_{\perp} = 6$ and various values of the parameter A as follows

A	$(E \, d^3\sigma/d^3p)_{weak}$ $(\Delta S=1)$
.5	$\sim 2 \times 10^{-37}$
1.0	$\sim 2 \times 10^{-38}$
1.5	$\sim 10^{-39}$
2.0	$\sim 10^{-40}$
2.5	$\sim .8 \times 10^{-41}$
3.0	$\sim 3 \times 10^{-43}$

As a result of these values we might expect a strong-weak interference effect of magnitude $\sim 10^{-37}$ cm^2/G^2_{ev} sterad. at a

$p_\perp$ of 6 Gev/c for values of $A < 1.5$. If the Λ^os produced by the weak interaction have a very large longitudinal polarization (~50 %) then we can observe these effects at these values of transverse momenta where a 10% measurement can be carried out. For values of $A > 1.5$ these effects become too small to be measurable.

In addition, we now expect the existence of a new class of particles in the mass region between 3 and 5 Gev. These are known as "charm particles"[8]. They are supposed to decay weakly and some will have a Λ^o in the final state. These Λ^os could exhibit a strong longitudinal polarization. Since their production cross section is expected to be comparable to the large P_T strong interactions, we should observe such effects in the region $2 \leq P_T \leq 4$ Gev/c.

We should point out that because of the spatial symmetry involved in p-p collisions, for particles produced at 90° in the center of mass, the polarization normal to the production plane must be zero.

Experimental Aspects

The detector must be so designed as to detect the presence of Λ^os of various momenta in a general background of unrelated particles. At the same time we must be able to measure systematic biases that the equipment may generate so as to remove them from the data. We discuss now the various aspects of measuring the Λ^o's decay parameters.

I) $\underline{\Lambda^o}$, $\underline{K^o}$ Separation - There are two neutral particles whose decays lead to oppositedly charged particles, the K^o and Λ^o. To separate these particles we must be able to measure the momenta and direction of their decay tracks so that we may, kinematically, distinguish the two.

In fig. 2 we show the opening angle of Λ^o and K^o_s decays as a function of $\cos(\theta_{cm})$ of the positive particle. Our expected angular resolution of 0.5 mrad and V momentum resolution of 5% will be sufficient to separate Λ's from K's for momenta less than 150 Gev/c. This can be seen more directly in fig. 3 where we show a Monte Carlo generation of the number of decays as a function of the opening angle for both K^o_s and Λ^o decays. These distributions assume a 10% V momentum resolution from measurement in our apparatus. The large bulk of small opening angle vees are Λ^os so that if the flux of Λ^os and K^os are equal as might be expected[7] we can use the opening angle criteria as one of the requirements for Λ^o identification. In fig. 4 we plot the opening angle of the vee versus the momentum of the slower particle. In the case of the K^o_s curve we use the slower of the two pions. Fortunately, in the region where the opening angle of the Λ^o and K^o decays are comparable, the momenta of the slower track is quite different for the 2 cases. The measuring accuracy needed to separate the two is about 0.5 mrads for the opening angle and about 2% for the momentum measurement. With this accuracy which is achievable we still have confusion between the 2 type of decays at the level of a few percent. This can be totally eliminated by the use of

Cerenkov counters which are necessary for a different experimental reason, to be discussed later.

To carry out the measurements discussed in the previous paragraph we need as part of our detector a V Spectrometer made up of drift chambers and multi-wire proportional chambers as described in our experimental apparatus section. The measuring accuracy of these chambers is described in the section entitled "Resolution".

The mass and momentum of the V can be determined according to the relation

$$P = P_2\theta \left\{\frac{1}{\theta_1} - \frac{\theta_2}{2}\right\}$$

$$M^2 = \theta \left\{ \frac{m_1^2}{\theta_2} + \frac{m_2^2}{\theta_1}\right\} + (p_2\theta)^2 \frac{\theta_2}{\theta_1}$$

where θ is the V opening angle and the indices 2 and 1 refer to the slow and fast particle respectively.

II) <u>General Particle Background</u> - Associated with the production of Λ^os and K^os at 80 mrads there are a large number of charged particles. In fig. 5 we present the calculated flux of charged particles expected at 80 mrads. to the incoming beam direction. This flux is a background that is desirable to remove with the use of a magnetic field. We are planning to use a 3 meter long sweeping magnet with a BL of 40 kGm. Using a neutral channel in this magnet with an opening of 1x1 cm^2 will allow us to remove all the charged particles below 50 Gev/c. Hence the charged particle background getting through the channel is very small (about one

particle per pulse). Therefore neutrons will be our major general background. Our detector must be a low mass device to reduce the number of neutron interactions. This is a basic property of our V spectrometer. The total amount of Mylar before our analyzing magnet is only about 30 mils (this is the major source of mass) giving a neutron interaction probability of $\sim 2 \times 10^{-3}$. This gives rise to about 10^3 interactions per sec. for neutrons with $p < 10$ Gev/c and a negligible amount for neutrons of higher momenta. We feel this is an acceptable background level for our detector. In additional we have a flux of gammas which can be removed by placing a few radiation lengths of lead at the entrance to the channel.

Since we are only interested in sweeping horizontally the particles near 80 mrads. and not the particles in the forward direction we propose to have a C type magnet, whose open edge is along ~80 mrads. to the forward direction. The rest of the volume we propose to fill with magnetized iron with a horizontal field direction so that particles are swept vertically. In this manner the high momentum particles in the forward direction will not be swept into the apparatus. Additional iron absorber can be placed as shown in fig. 1.

The number of particles that get through the total amount of iron absorber and strike our drift chambers which subtend a solid angle of 3×10^{-3} sterads. will consist mainly of muons that are not bent out by the magnetized iron. A very naive and straight forward calculation gives an upper

limit of 10^4 muons per sec will strike our detector for 10^{11} protons on target. This is still an acceptable background rate. We are presently carrying out a more detailed calculation of this source of background.

III) The Need for Cerenkov Counters - By now we know that the production of particles has a steep exponential dependence on the magnitude of the transverse momentum of the produced particle[4]. In order to be able to trigger on large transverse momentum Λ^os without being sensitive to the much more copious low transverse momentum Λ^os, we have added to our V spectrometer two Cerenkov Counters and 3 small scintillator hodoscopes as shown in fig. 1.

The purpose of these Cerenkov counters is to optimize the detection of high momentum Λ^os by measuring the fast proton from the Λ^o decay. The first of these Cerenkov counters (C_π) is set to detect pions with $P > 20$ Gev/c while it will not detect protons with $P < 110$ Gev/c. The other (C_p) is set to detect protons with $P > 40$ Gev/c. Their characteristics and detection efficiency will be discussed in the section describing the detector.

IV) Systematic Experimental Biases and the Precession of the Λ^o Spin - Because we are looking for an asymmetry in the center of mass angular distribution of the Λ^o decays we must understand all systematic biases in our detector that could lead to such an effect. All geometrical biases will be calculated by Monte Carlo Techniques. In addition, since the K^o decays can not have an asymmetry in their decay

angular distribution, we can use their decays as a means of monitoring systematic biases in our detector. Monte Carlo studies have shown that the K° and Λ° decay particles traverse similar regions of the V detector. Hence any malfunction of a region of the detector will produce asymmetries in the decay angular distribution of both K° and Λ° decays and hence can be corrected. In addition, we plan to monitor the efficiency of our Cerenkov counters as a function of particle momenta by latching them when they are not in the trigger as we will discuss in the section entitled "Data Taking Plan".

One of the most important methods we have to test the accuracy of our observation is the ability we have to <u>precess the Λ° spin</u>. If the Λ° is polarized in the plane of production (a parity violating state) then the vertical field from the "C type" sweeping magnet near the target will precess the Λ° spin in this plane. We plan to use this precession to study possible systematic effects by reversing the direction of the sweeping field. The precession angle is given by

$$\theta = \frac{2\mu_\Lambda}{h} \frac{eh}{2m_p c} \frac{BL}{c}$$

$$= 50^\circ \text{ for } BL = 40 \text{ kG-m.}$$

This angle is sufficiently large to determine whether any longitudinal polarization effects we observe follow the precession of the spin when we reverse the magnetic field.

By using all the checks discussed so far we should be able to subtract systematic effects in our detection efficiency which may give rise to a false longitudinal polarization signal.

V) <u>Λ° from Ξ Decays</u> - Because the Ξ^-, Ξ° decay weakly, the Λ°s from their decay are longitudinally polarized in the center of mass of the Ξ. We have studied the behavior and magnitude of this polarization and we discuss here our conclusions. At low transverse momenta the production cross section of the cascades is much smaller than the Λ° production cross section[9]. We, in addition, have carried out an analyses to indicate how many Λ°s from Ξ will enter our apparatus. In fig. 6(B) we plot the percentage of Ξ^- decays which occur before they are swept out by the C magnet right after the target and whose Λ°s break up in our decay region. As can be seen this number is very small and hence can be corrected for. In fig. 6(A) we show the percentage of Ξ° decays where both the Ξ° and Λ° break-up in our decay region. Since this is quite comparable to the number of direct Λ°s (discussed in the section entitled "V Detection Efficiency") we must discuss this decay more extensively.

The polarization of Λ°s from Ξ decays in the center of mass of the Ξ is given by the expression

$$P_\Lambda \propto \{-\alpha+|P_\Xi|(1-\gamma)\cos\theta\}\, k_\Lambda + \gamma\, P_\Xi - \beta(P_\Xi \times k_\Lambda)$$

where P_Ξ is the polarization of the cascade, k_Λ is the momentum of the Λ°, θ is the center of mass decay angle and α, β, γ are -.44, .32, .84 respectively. Since we observe all the Λ°s independent of decay angle we get the average polarization

$$P_\Lambda = -\alpha\, k_\Lambda + \gamma\, P_\Xi - \beta\int_{-1}^{1}(P_\Xi \times k_\Lambda)\, d\cos\theta$$

The polarization of these Λ°s will not change direction as we change the direction of the B field in the sweeping magnet unless the Ξ is also polarized in the production plane, namely P_{Ξ} is not zero. Hence the component of Λ° polarization which does not change by an angle $(2x50)^{\circ}$ as we change the direction of the sweeping field can be attributed to Λ°s from unpolarized Ξ which break up in our decay region. This should be sufficient to calculate directly the effect this will have on Λ°s from Ξ° that decay within the region of the sweeping magnet.

In addition we have studied the detection of gammas from the π°s produced in Ξ° decays and have designed a detector to observe them. The discussion of the detection efficiency of these gammas will be discussed in the section entitled "The Gamma Detector". Since the Λ°s from Ξ decays are produced at a reasonably large angle to the forward direction ($\sim$3 mrads. for 50 Gev/c Ξ) quite a few of these will not project back to the target when reconstructed. We are presently studying whether the resolution of our V spectrometer is adequate to observe this effect. Hence, it is quite possible that, with the checks described in this section, we may not need to construct the gamma detector which we will describe for the sake of completeness.

The Detector

We have discussed so far the requirements we must meet to successfully measure the Λ° decay angular distribution.

Our detector is shown schematically in figure 1 and the dimension of the various elements is presented in table 2. We now describe briefly each section of the detector.

A) Sweeping Magnet and Shielding - Right after the target we plan to install a series of sweeping magnet sections. A sectional (like a C type) magnet that will sweep charged particles in the horizontal plane but only in the region near the neutral channel at 80 mrads. Looking from the target downstream, this magnet would be to the right of beam direction. To the left of this magnet which covers the front and left of the interaction region we would place 3 meters of magnetized iron with the field in such a direction as to sweep particles in a vertical direction. After this first 3 meters we would place another 3 meters of magnetized iron to sweep the particles further in the vertical plane. A magnetic field near 10 kG. in a cross sectional area of 30x30 cm^2 would be sufficient. It may be desirable to add more shielding along the left side of the decay region (as shown with dashed lines in fig. #1) where the background might be more severe. This can be carried out after we determine the background level.

B) The Neutral Channel - In the "C magnet" area we propose a neutral channel with an opening at the end of 1x1 cm^2 giving rise to a solid angle at the end of the 3 meters of $10^{-4}/9 \simeq 10^{-5}$ sterad. This solid angle is designed for 10^{11} protons on target.

At the entrance to this neutral channel we would like to be able to locate up to 10 radiation lengths of Pb in steps

of 2 radiation lengths to remove the gamma component of the neutral beam. This should be carried out by remote control.

C) The Decay Region - The Λ^os and K^os are allowed to decay in an 8 meter evacuated area. The opening at the far end of the decay region has a circular dimension of 25 cm. in radius and at the front end about 7 cm. in radius. The windows will consist of 10 mils of Mylar. The multiple scattering of a 10 Gev/c particle in the Mylar is 0.06 mrads. which is quite small compared to the needed resolution of 0.5 mrads. At the beginning of the decay region we plan to locate a small multi wire proportional chamber to anti all charged particles going into the detector ($\sim$ 3x3 cm^2).

D) The V Spectrometer - This spectrometer will consist of drift chambers for good spatial and angular resolution, multi-wire proportional chambers for good time resolution and an analyzing magnet to measure the momenta of the V decay tracks.

The drift chambers will consist of modules each of which has 2X and 2Y chambers. Each chamber will have readout wires 2 cm apart or 1 cm drift space. The size of these chambers is 60x60 cm^2. Each of the 2X and 2Y chambers will be shifted relative to one another by half the wire spacing to resolve the left-right ambiguity associated with these devices. We plan to achieve a 2 nsec. time resolution in the drift time giving us a 100 micron spatial resolution[6]. A picture of such a drift chamber built here is shown in fig. 7. There will be 4 such modules, 2 in front and 2 in back of the analyzing magnet. The distance between modules is 1 meter giving rise to an angular resolution of $\sim 10^{-4}$ radians.

We propose to use 4 MWPC. Two of them will be UV planes between the drift chambers to resolve double track ambiguities. We propose to place one MWPC just before the analyzing magnet and one at the end of the V detector. The wire spacing will be 2mm. These chambers will be used as part of the trigger. The MWPC's have a time resolution of 50 nsec but a spatial resolution of only 1 mm , in contrast with drift chambers which need time spreads of 200 nsec but have a spatial resolution of 0.1 mm. Therefore, the combination of the MWPC and drift chamber will optimize our spatial and time resolution while reducing the amount of material in the detector to a minimum.

The analyzing magnet is proposed to have an aperture of 70x60 cm^2 and be 1 meter long. The maximum field necessary is 15 kG.

E) <u>The Proton Detector</u> - To optimize the detection of high momentum Λ^os we propose to measure the momentum of the proton from the Λ^o decay. The detector will consist of 3 scintillator counter hodoscopes SH_1, SH_2, SH_3. Between these hodoscopes there will be 2 Cerenkov counters. One is a 10 meter long He gas counter to detect pions with $P > 20$ Gev/c and the other a 1.5 meter long CO_2 gas counter to detect protons with $P > 40$ Gev/c. Protons with $P < 110$ Gev/c will not trigger the He counter. The characteristics of these Cerenkov counters are standard and are shown in figs. 8 and 9. In fig. 10 we plot the trigger efficiency which is the Poisson probability of having one or more photoelectrons.

F) <u>The Gamma Detector</u> - In order to detect the gammas from Ξ° decays we have 2 arrays of 6"x6"x8" (21 pieces) lead glass counters $(LGH)_1$ and $(LGH)_2$. The first hodoscope covers an area of 24"x24" around the SH_1 hodoscope and the second covers an area 12"x12" behind the SH_3 hodoscope. In fig. 11 we present the detection efficiency of the gammas from Ξ° decays whch trigger our detector with its Λ° decay. We present both the probability of detecting one or two γs (A) and the probability of detecting both γs (B). In fig. 12 we present the momentum distribution of these gammas. At these energies (above $E_{\gamma} > 1$ Gev) the energy resolution of lead glass counters is given by FWHM = $(1.5 + 10/\sqrt{E})\%$[10] indicating an energy resolution of about 6%. In this manner we can measure the longitudinal polarization of Λ°s when it is associated with a gamma in this energy range. We can then determine whether this polarization is consistent with the polarizations expected from Ξ decays.

Resolution

Because of the use of drift and multi-wire Proportional Chambers the time and spatial resolution of the decays are well determined. We can require that the decay tracks cross our chambers within 50 nsec of each other and that the position in the drift chamber agree with the MWPC position giving us a 1 mm. spatial resolution. Because the drift chambers are capable of giving 100 micron spatial resolution, Monte Carlo studies have shown that the decay point of the V can be determined to ±25 cm and that the distance of

closest approach of the 2 tracks is better than 0.25 mm. Using the projected cross sectional area of the beam as the source of the V we can determine the direction of the V to better than 0.5 mrads, which is similar to the accuracy with which we can determine the direction of the decay tracks. Hence we are able to measure all angles involved in a V decay to about 0.5 mrads. The momenta of the least energetic particle is measured to a few percent while that of the more energetic track to about 10%.

We plan to use the spatial resolution of the 2 crossing tracks in our decay volume as additional constraints to determine the presence of a V. This requirement in addition to the kinematic constraints of a V decay and the Cerenkov Counter trigger should be sufficient to remove all possible background.

Finally, in fig. 16 we present the accuracy with which we can measure the polarization as a function of P_T.

V Detection Efficiency

We have made a Monte Carlo simulation of our apparatus to determine its V detection efficiency. In fig. 13 we show the percentage of charged decays (branching ratios included) that will occur in our 8 meter decay region for various sweeping magnet dimensions. In fig. 14(A) we show the apparatus detection efficiency for Λ^os which break up in the decay region under two running conditions. The solid curve refers to the efficiency when we run with the analyzing magnet at 15 kG.

and the trigger requirement being

$$\text{EVENT} = (>2 \text{ in MWPC})\ (SH_1)\ (\overline{\check{C}_\pi})\ (SH_2)\ (\check{C}_p)\ (SH_3)$$

The dashed curve refers to the condition B = 7.5 kG. and the same trigger requirement without the proton Cerenkov counter in the trigger. Because of the exponential behavior of large P_T particle production, we need a sharp trigger requirement that will allow us to trigger only on large P_T Λ^os without recording the much more numerous low P_T Λ^o decays. This sharp requirement is achieved by the efficiency represented in our solid curve. Fig. 14(B) represents the percentage of Λ^os produced at the target that will trigger our detector.

In figs. 15(A) and 15(B) we plot the same curves when applied to K^o decays. Here the Cerenkov cut off is the effect of putting the $\check{C}_\pi$ Cerenkov in coincidence with the scintillation counter trigger $(SH_1)(SH_2)(SH_3)$. In this case the effect of the Cerenkov is seen to be minimal and hence not useful.

Data Taking Plan

We propose to take our data under 2 running conditions. One with the analyzing magnet at 15 Kg. and both the Cerenkov counters in our trigger (i.e. trigger on "EVENT"). In this manner we will trigger only on high P_T Λ^o decays. We plan to spend most of our time in these running conditions. Interspersed with these large blocks of time will be short running periods where the analyzing magnet is at 7.5 kG. and the Cerenkov counters are not in the trigger but are still latched.

These periods will record the low momentum Λ^os and the K^os decays. The study of K_s^o decays besides giving good data will also be used to study the geometrical biases of our apparatus and the trigger efficiencies of our Cerenkov counters. In this manner by running these short periods often we can monitor the performance of our apparatus.

Expected Λ^o Rates

In table 1 we show the expected Λ^o fluxes to be recorded by our detector per pulse under our two running conditions. The K^o fluxes are similar. The assumption made in obtaining these results is that these fluxes are one half the pion fluxes as measured by J. W. Cronin et. al.[4]. These fluxes should allow us to detect a 10% polarization for $P_T \sim 6$ Gev/c at 300 Gev/c beam momentum. This implies measuring the longitudinal polarization down to production cross sections of 10^{-36} cm^2. If we run for a period of 400 hours or ~20 days we can determine the polarization at 10^{-36} cms^2 with an error of ~0.1.

We are requesting a running period of 700 hours, about 300 hours for testing at low and medium intensities and the rest with 10^{11} protons on target at 300 Gev/c. This request is based on an accelerator rep. rate of 6 pulses/minute.

Future Group Commitments

At present some of us are committed to carry out a test run in collaboration with L. Pondrom and collaborators of Michigan and Rutgers. This is experiment number E415. One

of us (D.B.) has a magnetic monopole search. Both of these are short range commitments. Beyond this there are no further commitments to long range programs. At the same time we are actively looking for collaborators.

Equipment Needs

Colorado proposes to build the decay pipe, the drift and multi-wire proportional chambers and associated electronics. We also propose to build the scintillator hodoscopes and lead glass hodoscope if they are necessary. We request that FNAL contribute the shielding, sweeping magnet and analyzing magnet. We are planning to acquire on loan the Cerenkov counters that we need or try to get our future collaborators to contribute them. We expect to request a reasonable amount of fast electronics from PREP. The cost estimate for the equipment is shown in table 3.

Table 1

θ = 80 mrads.

Assume $\frac{Ed^3\sigma}{d^3p}_{(K^\circ,\bar{K}^\circ)} \approx \frac{Ed^3\sigma}{d^3p^3}_{\Lambda^\circ} \approx .5 \frac{Ed^3\sigma}{d^3p}_{\pi^\pm}$

P(Gev/c)	P_t	$Ed^3\sigma/d\ p$(200 Gev/c)	Detection (1)	Efficiency(Eff) (2)
10	.8	1.0×10^{-27}	0	0
20	1.6	4.0×10^{-29}	.01	0
30	2.4	1.0×10^{-30}	.135	0
40	3.2	0.8×10^{-31}	.20	.10
50	4.0	2.2×10^{-33}		.240
60	4.8	0.7×10^{-34}		.270
70	5.6	0.7×10^{-35}		.290
80	6.4	3.0×10^{-37}		.292

$\Delta\Omega = 1.1\times10^{-5}$

$\sigma_T(pp) = 40$mb.

f = fraction of interacting beam = 0.4

$N(p) = 10^{11}$/pulse

$\frac{\Delta p}{p} = 0.15$(~ binning size)

$$\text{Flux/pulse} = N(p)\ \frac{Ed^3\sigma/d^3p}{\sigma_T}\ (\Delta\Omega)(p^2)(\frac{\Delta p}{p})(f)(\text{Eff})$$

$$= \frac{10^{11}}{40}\ \frac{Ed^3\sigma/d^3p}{10^{-27}}\ \text{x}\ 1.1\text{x}10^{-5}\ p^2\text{x}.15\text{x}.4(\text{Eff})$$

$$= \frac{1.1\text{x}.15\text{x}.4}{40}\ \text{x}\ 10^6\ \frac{Ed^3\sigma/d^3p}{10^{-27}}\ p^2(\text{Eff})$$

$$= 1.1\text{x}.15\text{x}10^4$$

$$= 1.6\text{x}10^3\ \frac{Ed^3\sigma/d^3p}{10^{-27}}\ p^2(\text{Eff})$$

P(Gev/c)	P_t(Gev/c)	Λ°Flux (200 Gev/c incident protons)/pulse (1)	(2)
10	.8	0	
20	1.6	250	
30	2.7	190	
40	3.2	40	20
50	4.0		2.1
60	4.8		$1.1\text{x}10^{-1}$
70	5.6		$1.6\text{x}10^{-2}$
80	6.4		$9.0\text{x}10^{-4}$

Table 2

Detector Dimensions and Details

a) Sweeping C type Magnet	
Cross Sectional Area	~30x30 cm^2
Length	3 meters up to 5 meters
BL necessary	40 kg meters
b) Shielding Forward Direction	
Cross Sectional Area	~50x50 cm^2
Length	~6 meters
BL requested	~40 kg meters
c) Decay Region	
Length	8 meters
Downstream Opening Diameter	50 cms.
Upstream Opening Diameter	14 cms.
d) Drift Chambers	
Cross Sectional Area	60x60 cm^2
Chamber Spacings	1 meter
Readout Wire Spacing	2 cms.
Maximum Drift Distance	1 cm.
Maximum Drift Time	200 nsec.
Desired Spatial Resolution	0.1 mm.
e) Multi-Wire Proportional Chambers	
Cross Sectional Area	60x60 cm^2
Wire Spacing	2 mm.
Time Resolution	50 nsec.
Spatial Resolution	1 mm.

f) Analyzing Magnet

Cross Sectional Area	60x70 cm^2
Length	1 meter
Maximum Field Desired	15 kg.

g) Scintillator Hodoscope Counters

Cross Sectional Area	
SH_1	14x10 cm^2
SH_2	36x20 cm^2
SH_3	46x20 cm^2
Thickness	1/8"

h) Cerenkov Counters

1) $\check{C}_\pi$

Length	10 meters
Diameter	36 cms.
Gas fill	He up to 1.4 atm.

2) $\check{C}_p$

Length	1.5 meters
Diameter	40 cms.
Gas fill	CO_2 up to 1.4 atm.

i) Lead Glass Hodoscope (may not be necessary)

1) SH_1

Inner Dimension	14x10 cm^2
Outer Dimension	60x60 cm^2
Unit block size	6"x6"x8"

2) SH_2

Inner Dimension	0
Outer Dimension	40x30 cm^2
Unit block size	6"x6"x8"

Table 3

Cost Estimate

1)	Decay Pipe	$ 3000
2)	16 Drift Chambers at 32 readout wires/chamber	
	Construction ($500/chamber)	$ 8000
	Electronics ($50/wire)	$26000
3)	4 MWPC at 300 wires/chamber	
	Construction ($500/chamber)	$ 2000
	Electronics ($10/wire)	$12000
4)	Scintillator Hodoscopes	
	Material and Labor	$ 2000
	15 Phototubes (to be borrowed if possible)	$ 4500
5)	2 Cerenkov Counters (to be borrowed if possible)	$20000
6)	High Speed Electronics (Hopefully a lot from PREP)	
	20 Discriminators	$10000
	10 Coincidence Units	$ 8000
	5 Visual Double Scalers	$ 3000
	40 Latches	$ 8000
7)	On Line PDP 11 Computer	$30000
8)	Camac Modules	$20000
9)	Analyzing Magnet	?
10)	Sweeping Magnet	?

References

1) See 1973 POPAE Summer Study, 1974 PEP Summer Study and BNL Report #17522.

2) There are many references on this subject. Some of these are S. B. Berman, J. D. Bjorken, and J. B. Kogut; Phys. Rev. D-4, 3388 (1971). R. Blankenbeckler, S. J. Brodsky, and J. F. Gunion; Phys. Letters 42B, 461 (1972). P. V. Landshoff and J. C. Polkinghorne; Phys. Letters 45B, 361 (1973). S. D. Ellis and M. B. Kislinger; NAL Report No. PUB-73/40/THY (to be published). G. R. Farrar; CALTEC Report No. CALT-68-422 (to be published). H. P. Paar and E. A. Paschos (to be published in Phys. Rev.). R. Savitt and M. B. Einhorn; Phys. Rev. Letters 33, 392 (1974).

3) M. Banner, J. L. Hamel, J. P. Pansart, J. V. Stirling, J. Teiger, H. Zaccone, J. Zsembery, G. Bassompierre, M. Croissiaux, J. Gresser, R. Morand, M. Riedinger, M. Schneegans, Phys. Letters 41B, 547 (1972) and Phys. Letters 44B, 537 (1973). A. Bertin, P. Capiluppi, M. D'Agostini-Bruno, R. J. Ellis, G. Giacomelli, A. M. Rossi, and G. Vannini, A. Bussiere, R. T. Poe, Phys. Letters 42B, 493 (1972). B. Alper, H. Boggild, G. Jarlskog, G. Lynch, J. M. Weiss, P. Booth, L. J. Carroll, J. N. Jackson, M. Prentice, G. Von Dardel, L. Jonsson, G. Damgaard, K. H. Hansen, E. Lohse, F. Bulos, L. Leistam, A. Klovning, E. Lillethun, B. Duff, F. Heymann, and D. Quarrie, Phys. Letters 44B, 521 (1973). B. Alper, H. Boggeld, G. Jarslskog, J. M. Weiss, P. Booth, L. J.

Carroll, J. N. Jackson, M. Prentice, G. von Dardel, G. Damgaard, F. Bulos, W. Lee, G. Manning, P. Sharp, L. Leistam, A. Klovning, E. Lillethun, B. Duff, K. Potter, D. Quarrie and S. Sharrock, Phys. Letters 44B, 527 (1973). F. W. Busser, L. Camilleri, L. DiLella, G. Gladding, A. Placci, B. G. Pope, A. M. Smith, J. K. Yoh, E. Savattini, B. J. Blumenfeld, L. M. Lederman, R. L. Cool, L. Litt, and S. L. Segler, Phys. Letters 46B, 471 (1973).

4) J. W. Cronin, H. J. Frisch, M. J. Shochet, J. P. Boymond, P. A. Piroue, R. L. Sumner, Phys. Rev. Letters 31, 1426 (1973). J. P. Boymond, R. Mermod, P. A. Piroue, R. L. Sumner, J. W. Cronin, H. J. Frisch, and M. J. Sochet, Phys. Rev. Letters 33, 112 (1974) and Papers submitted to the XVII International Conference in High Energy Physics. J. A. Appel, M. H. Bourquin, I. Gaines, D. C. Hom, L. M. Lederman, H. P. Paar, J. P. Repellin, D. H. Saxon, H. D. Snyder, J. M. Weiss, J. K. Yoh, B. C. Brown, J. M. Gaillard, and T. Yamanouchi, Phys. Rev. Letters 33, 719 and 722 (1974).

5) The factor 10 $\sin^2\theta$ is the factor that leads to the correct decay rate for the process $\Lambda^\circ \to p\pi^-$. Since this is a purely hadronic $\Delta S = 1$ weak vertex we assume this correction to the weak coupling also applies in our process. The factor of 10 necessary to correct the purely Cabibbo theory is known as "Octet Enhancement". We thank K. T. Mahanthappa for pointing this out.

6) This time resolution and linearity we have achieved in a drift chamber built by us. See also M. Atac, W. E. Taylor, Nuclear Instruments and Methods 120, (1974), 147.

7) We are making this assumption based on the observation that the number of protons and pions at large transverse momenta are almost the same. See Cronin et. al.[4]. Hence since $|S(K^\circ, \bar{K}^\circ)| = |S(\Lambda^\circ)| = 1$ we expect this ratio to be about the same.

8) M. K. Gaillard, B. W. Lee, J. L. Rosner Fermi Lab - Pub. 74/86 - THY and Review of Modern Physics Vol. 47, #2, 1975.

9) The Ξ° cross section is about 1% of the Λ° cross section. J. Steinberger et. al. CERN results. Also L. Pondrom et. al. seem to see very few cascades in their NAL experiment (preliminary results).

10) M. Holder, E. Radermacker, A. Stande, P. Darriulat, J. Deutsch, J. Pilcher, C. Rubbia, K. Kittel, C. Grosso-Pilcher, M. Seire, A. Villari, Nuclear Inst. and Methods 108, 541 (1973), and J. A. Appel, M. H. Bourquin, I. Gaines, D. C. Hom, L. M. Lederman, H. P. Paar, J. P. Repellin, D. H. Saxon, H. D. Snyder, J. M. Weiss, J. K. Yoh, B. C. Brown, C. N. Brown, J. M. Gaillard, J. R. Sauer, T. Yamanouchi. Preprint, to be published.

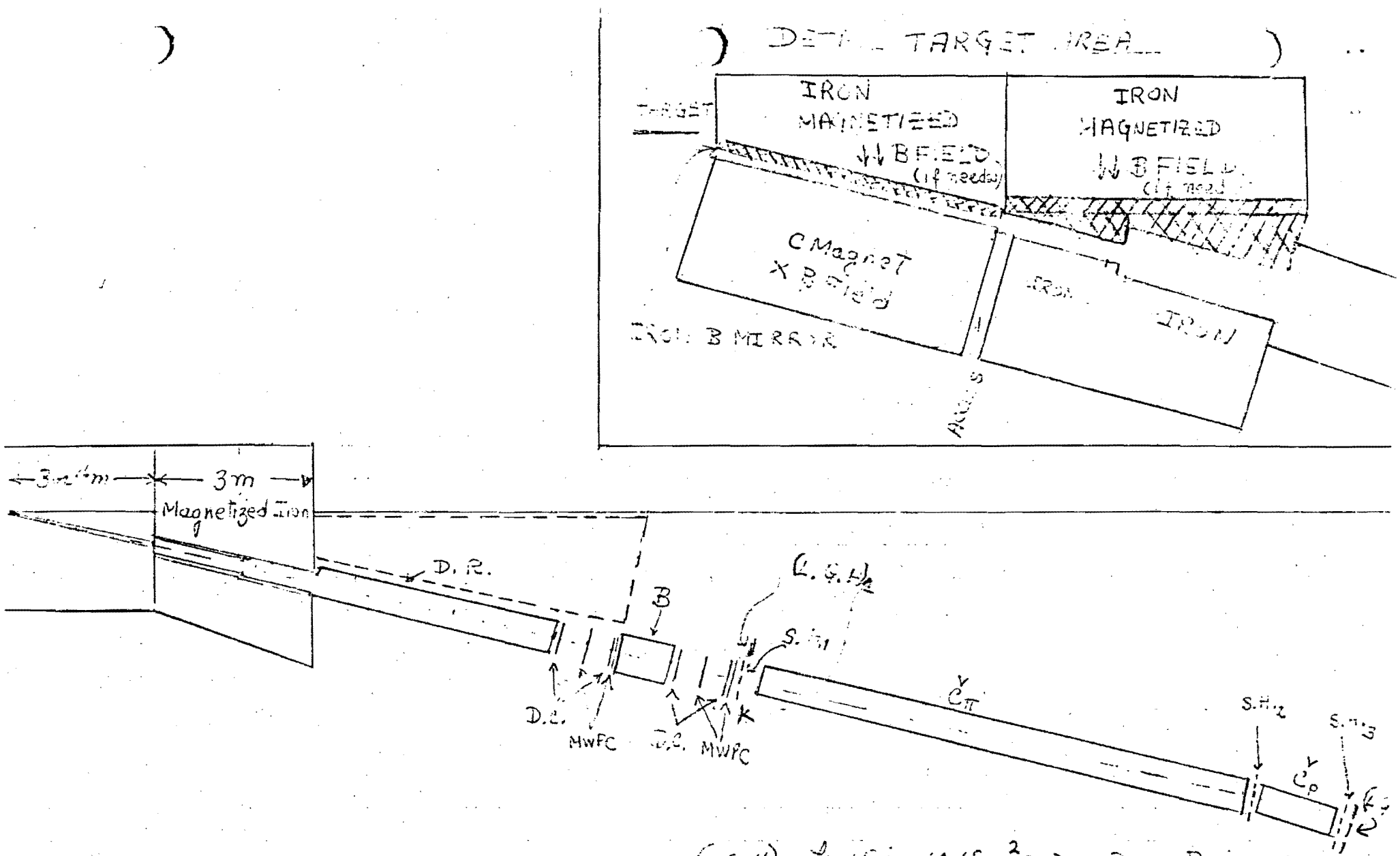

$(L.G.H)_1$ = Lead Glass 60x60 cm^2 D.R. = Decay Region = 8 m.
$(L.G.H.)_2$ = " " 40x30 cm^2 D.C. = Drift Chambers 60x60
S.H. = Scintillator Hodoscopes
SH_1 = 14x10x.3 cm^3
SH_2 = 36x20x.6 cm^3
SH_3 = 46x20x.6 cm^3
B = Analyzing Magnet 70x60x100
C_π = 10 m. [illegible]

Long. Dimension = 1m. = 1cm.
Trans. Dimension Arbitrary.

FIG 1.

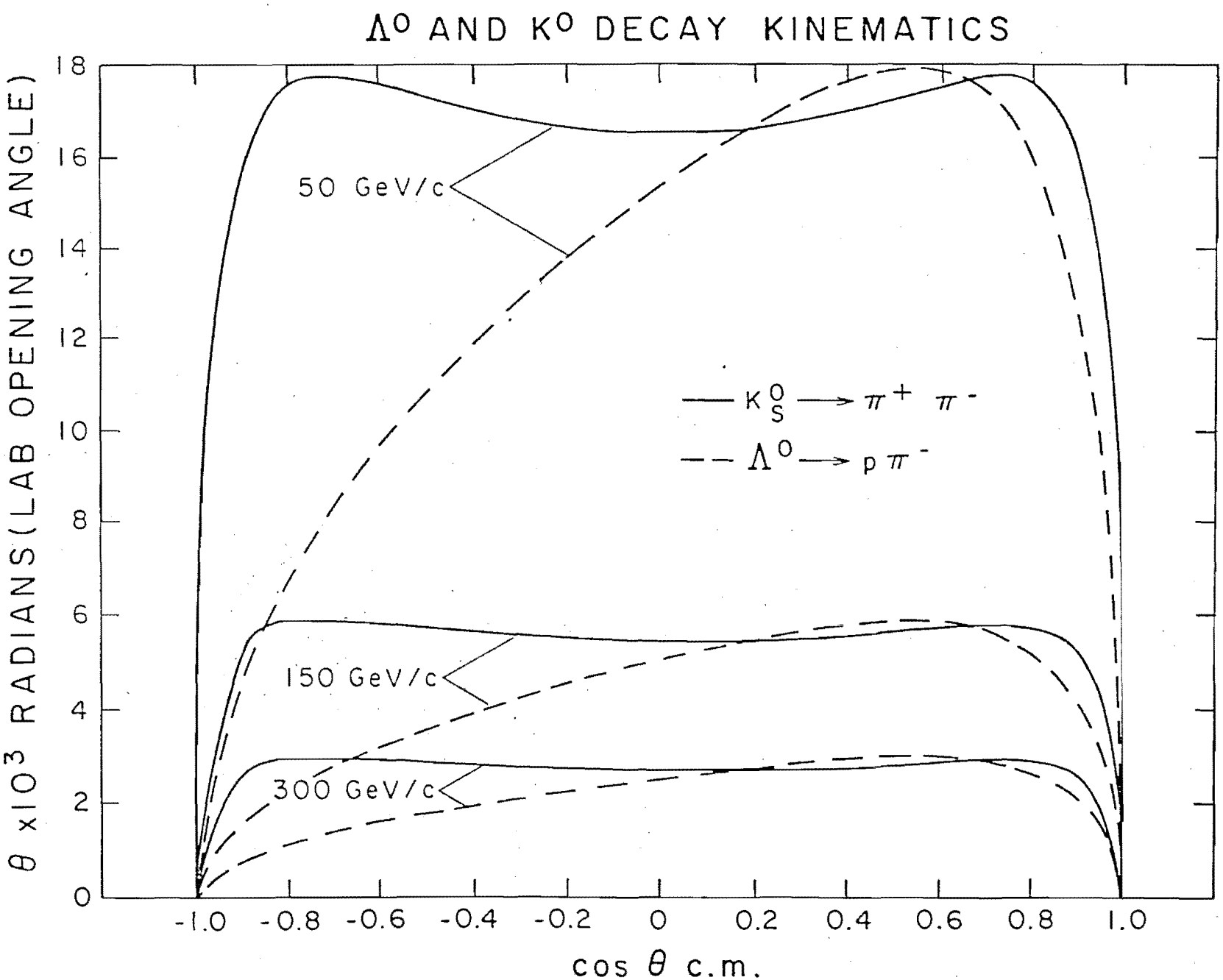
Λ0 AND K0 DECAY KINEMATICS
θ x10^3 RADIANS (LAB OPENING ANGLE)
18
16
14
12
10
8
6
4
2
0
50 GeV/c
150 GeV/c
300 GeV/c
K0S → π+ π-
Λ0 → p π-
-1.0
-0.8
-0.6
-0.4
-0.2
0
0.2
0.4
0.6
0.8
1.0
cos θ c.m.

Fig. 2

K+E 10 X 10 TO THE CENTIMETER 46 1510
18 X 25 CM MADE IN U.S.A.
KEUFFEL & ESSER CO.

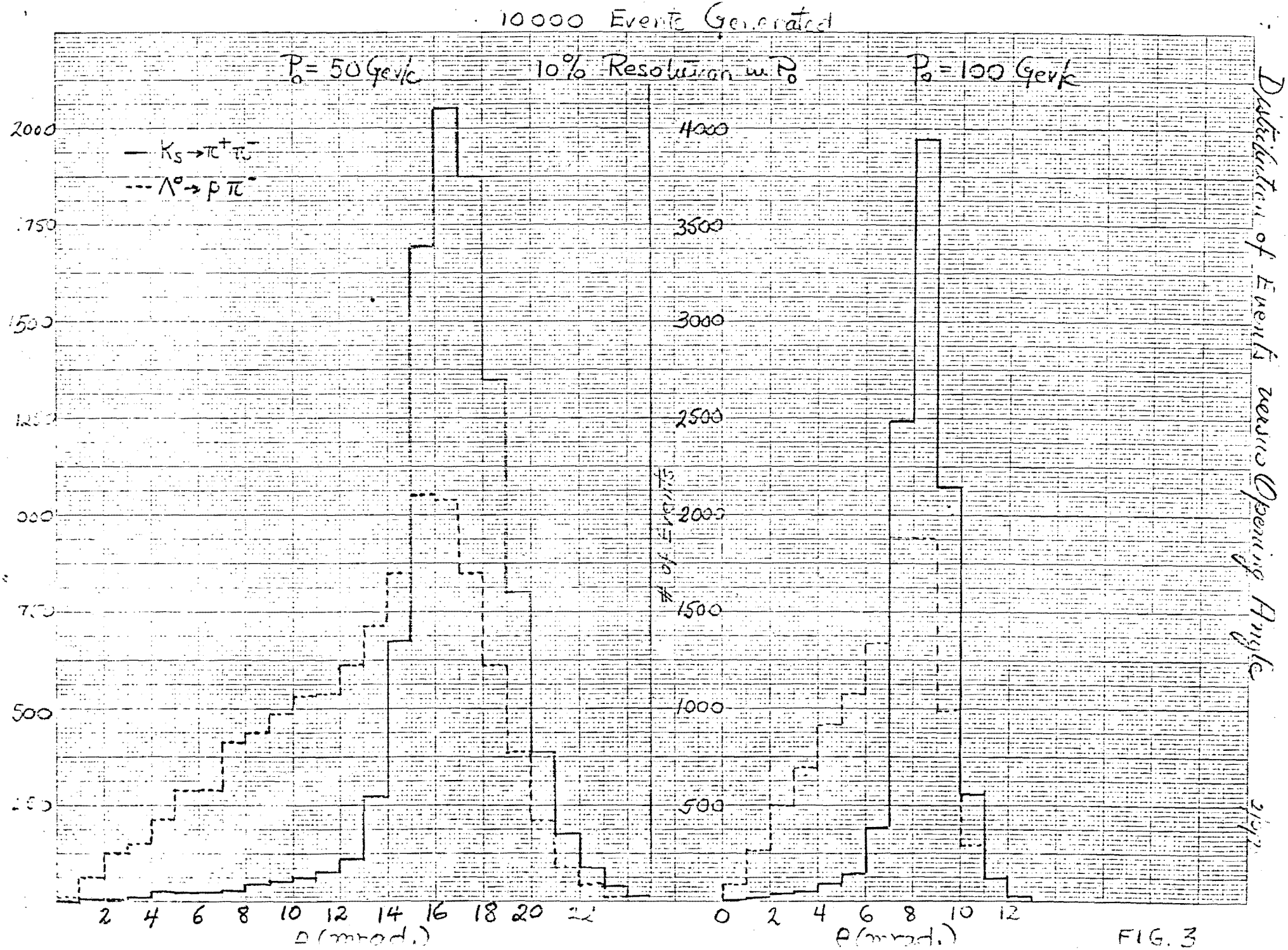

Distribution of Events versus Opening Angle

FIG. 3

10 X 10 TO THE CENTIMETER 46 1510
18 X 25 CM. MADE IN U.S.A.
KEUFFEL & ESSER CO.

Momentum of Slower Particle Versus Opening Angle

3/27/75

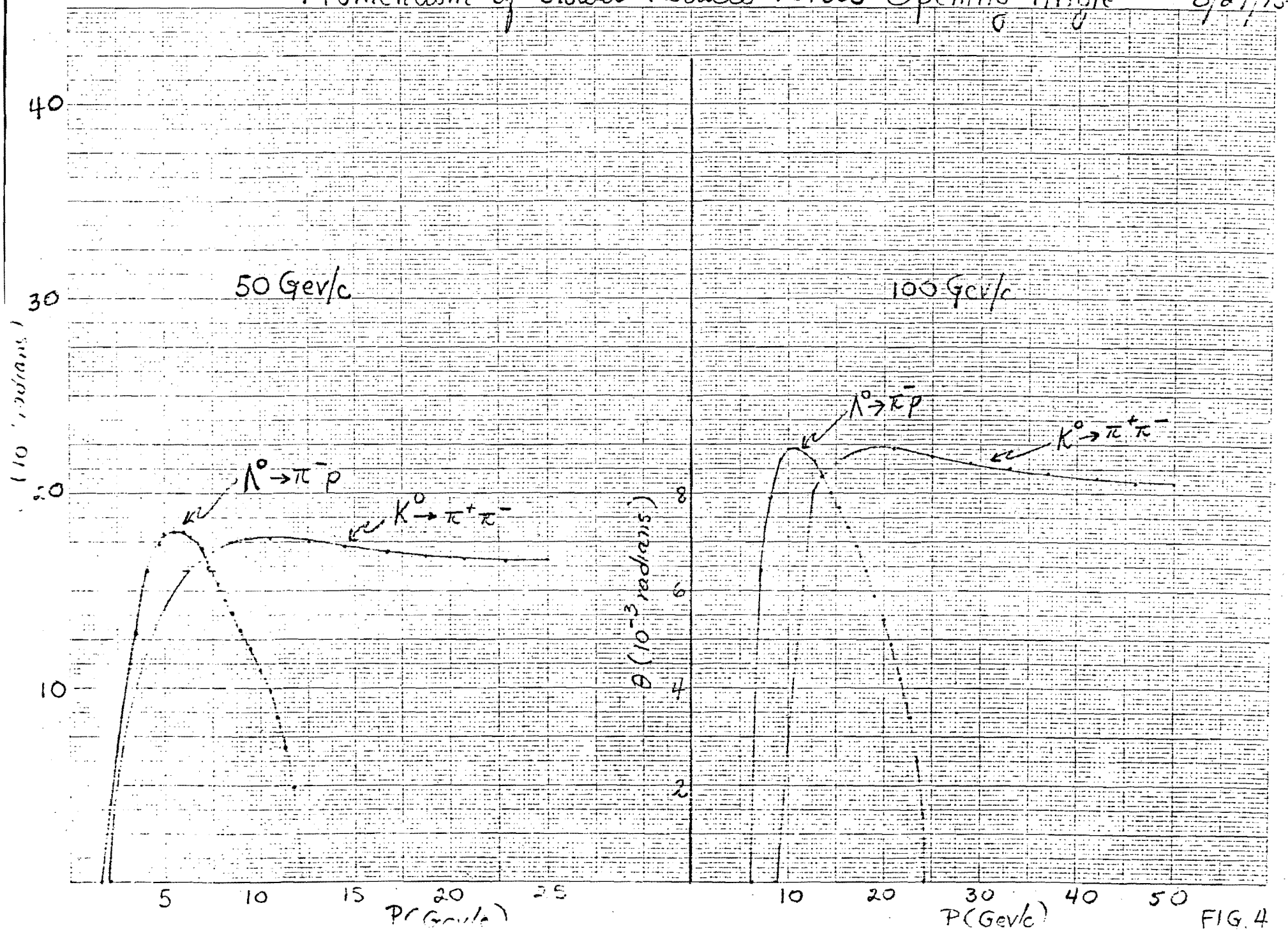

FIG. 4

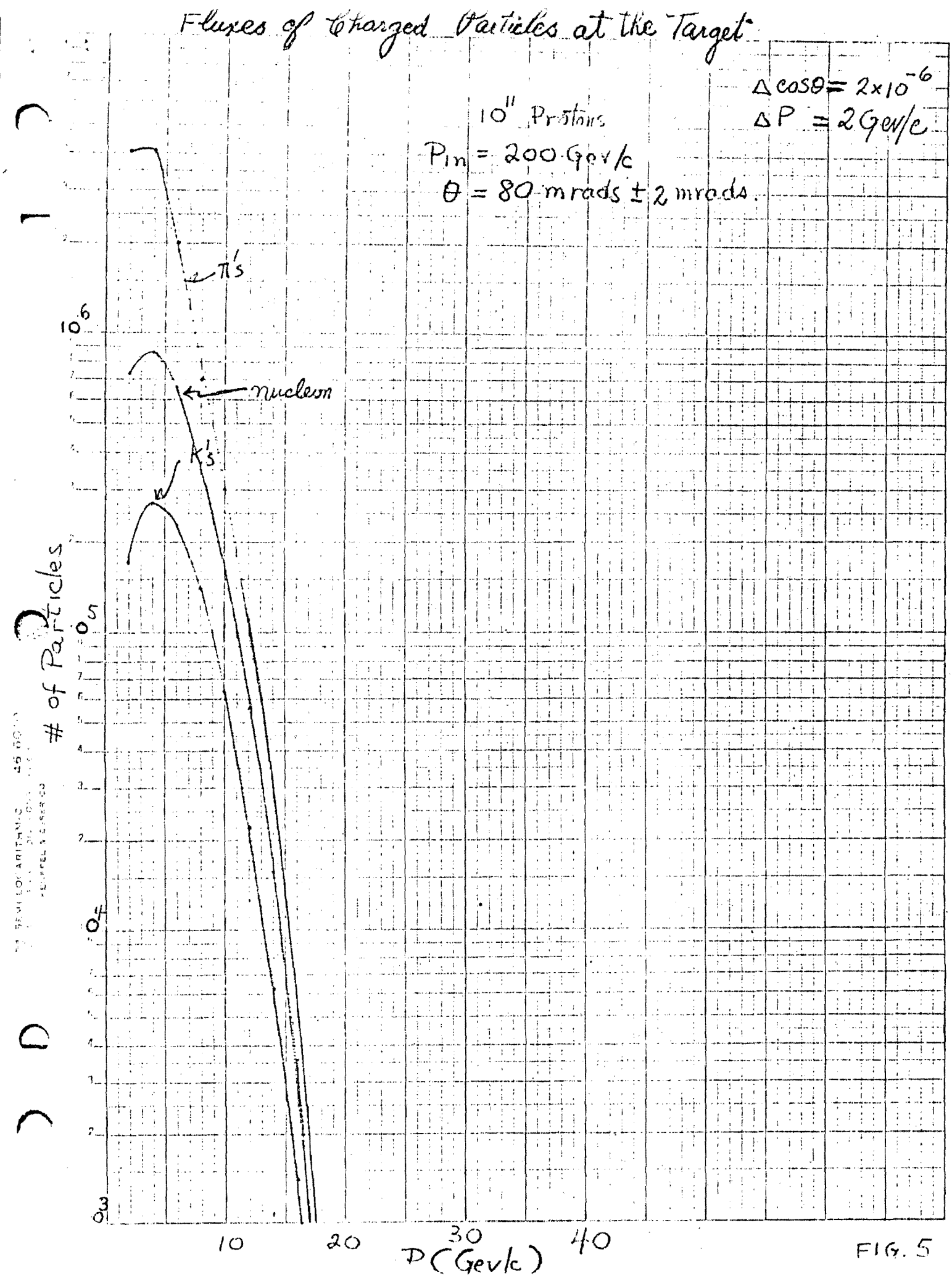
Fluxes of Charged Particles at the Target
$\Delta \cos\theta = 2\times10^{-6}$
$\Delta P = 2$ Gev/c
10^{11} Protons
$P_{in} = 200$ Gev/c
$\theta = 80$ mrads ± 2 mrads.
π's
nucleon
K's
# of Particles
10^6
10^5
10^4
10^3
10
20
30
40
P (Gev/c)

FIG. 5

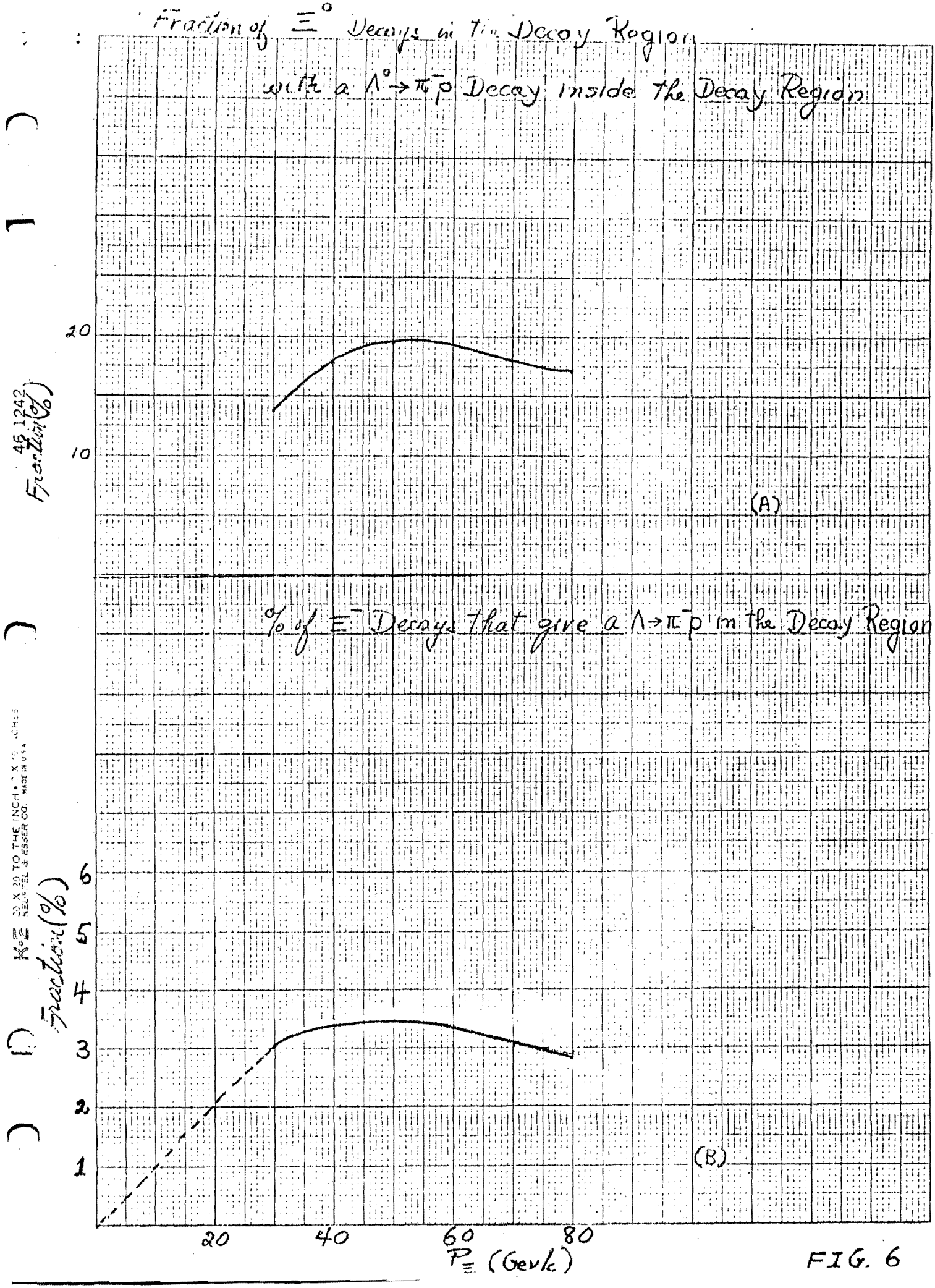
Fraction of Ξ^0 Decays in the Decay Region
with a $\Lambda^0 \to \pi^- p$ Decay inside the Decay Region
20
10
Fraction (%)
(A)
% of Ξ^- Decays that give a $\Lambda \to \pi^- p$ in the Decay Region
6
5
4
3
2
1
Fraction (%)
(B)
20
40
60
80
P_Ξ (Gev/c)

FIG. 6

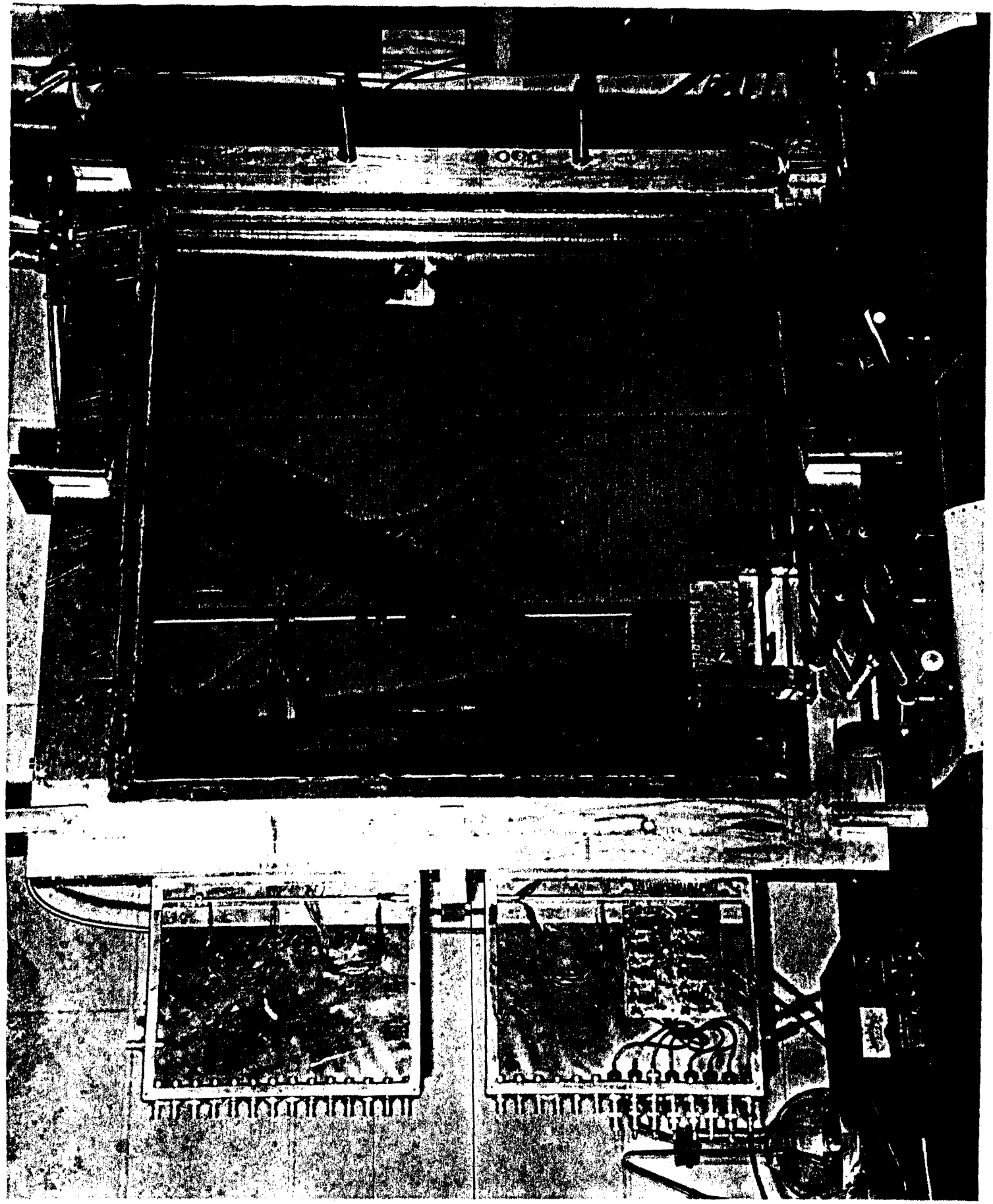

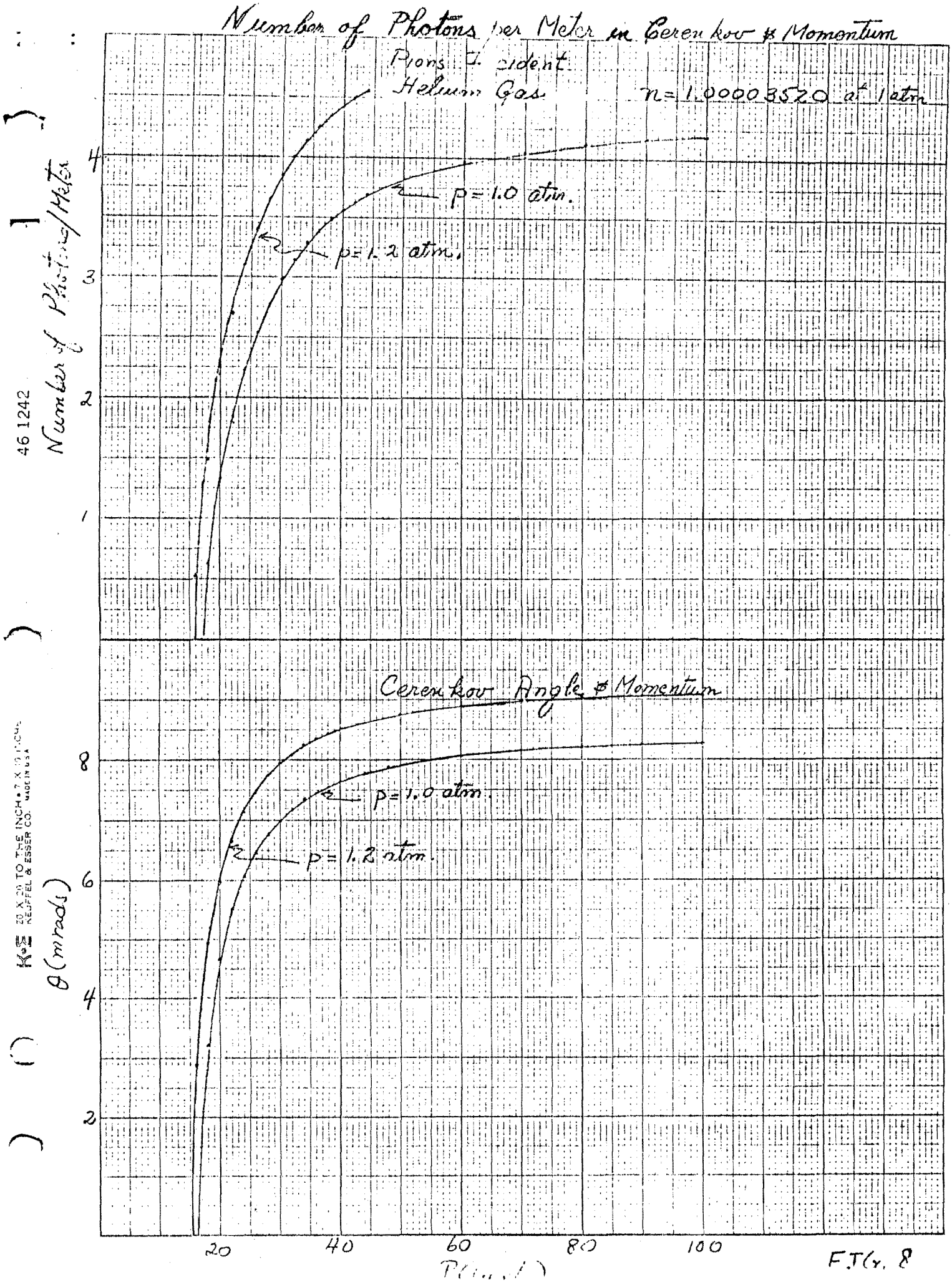
Number of Photons per Meter in Cerenkov & Momentum
Pions Incident
Helium Gas
n = 1.00003520 at 1 atm
p = 1.0 atm.
p = 1.2 atm.
Number of Photons/Meter
1
2
3
4
Cerenkov Angle & Momentum
p = 1.0 atm.
p = 1.2 atm.
θ (mrads)
2
4
6
8
20
40
60
80
100
46 1242
K+E 20 X 20 TO THE INCH • 7 X 10 INCHES
KEUFFEL & ESSER CO. MADE IN U.S.A.

FIG. 8

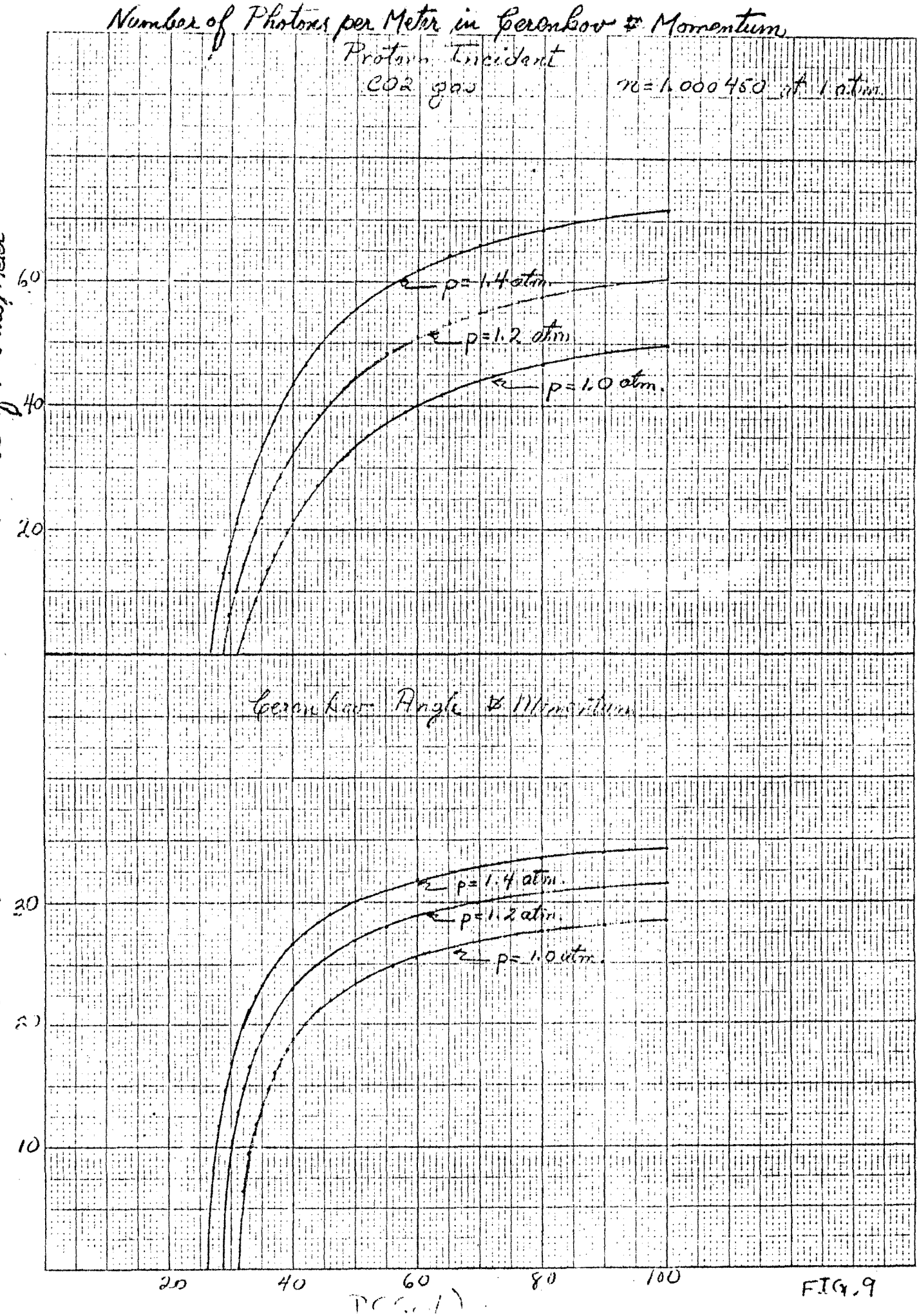

FIG. 9

46 1242
K+E 20 X 20 TO THE INCH • 7 X 10 INCHES
KEUFFEL & ESSER CO. MADE IN U.S.A.

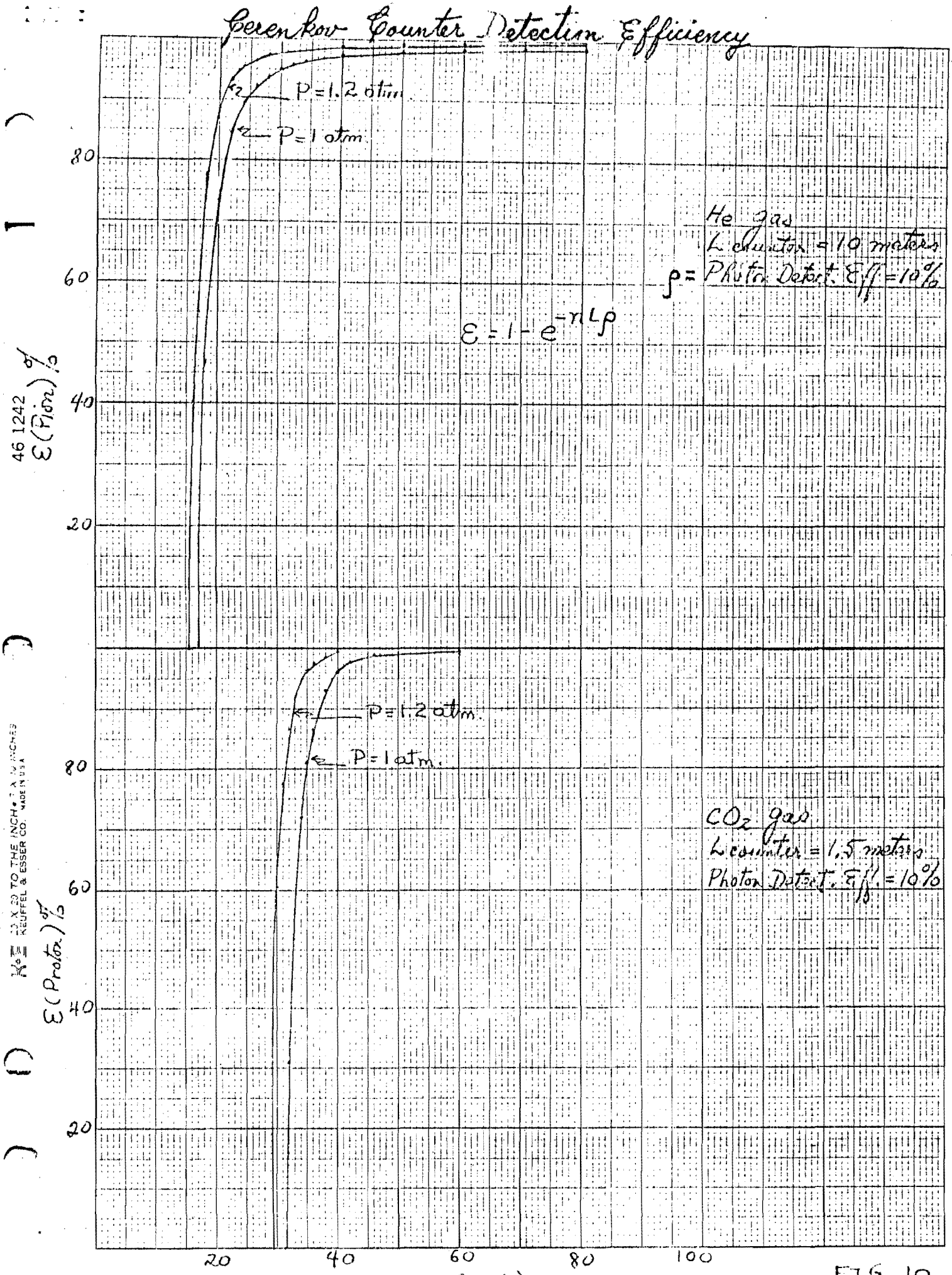
Cerenkov Counter Detection Efficiency
P = 1.2 atm
P = 1 atm
He gas
L counter = 10 meters
ρ = Photon Detect. Eff = 10%
ε = 1 - e^{-nLρ}
ε (Pion) %
80
60
40
20
P = 1.2 atm.
P = 1 atm.
CO2 gas
L counter = 1.5 meters
Photon Detect. Eff. = 10%
ε (Proton) %
80
60
40
20
20
40
60
80
100

FIG 10

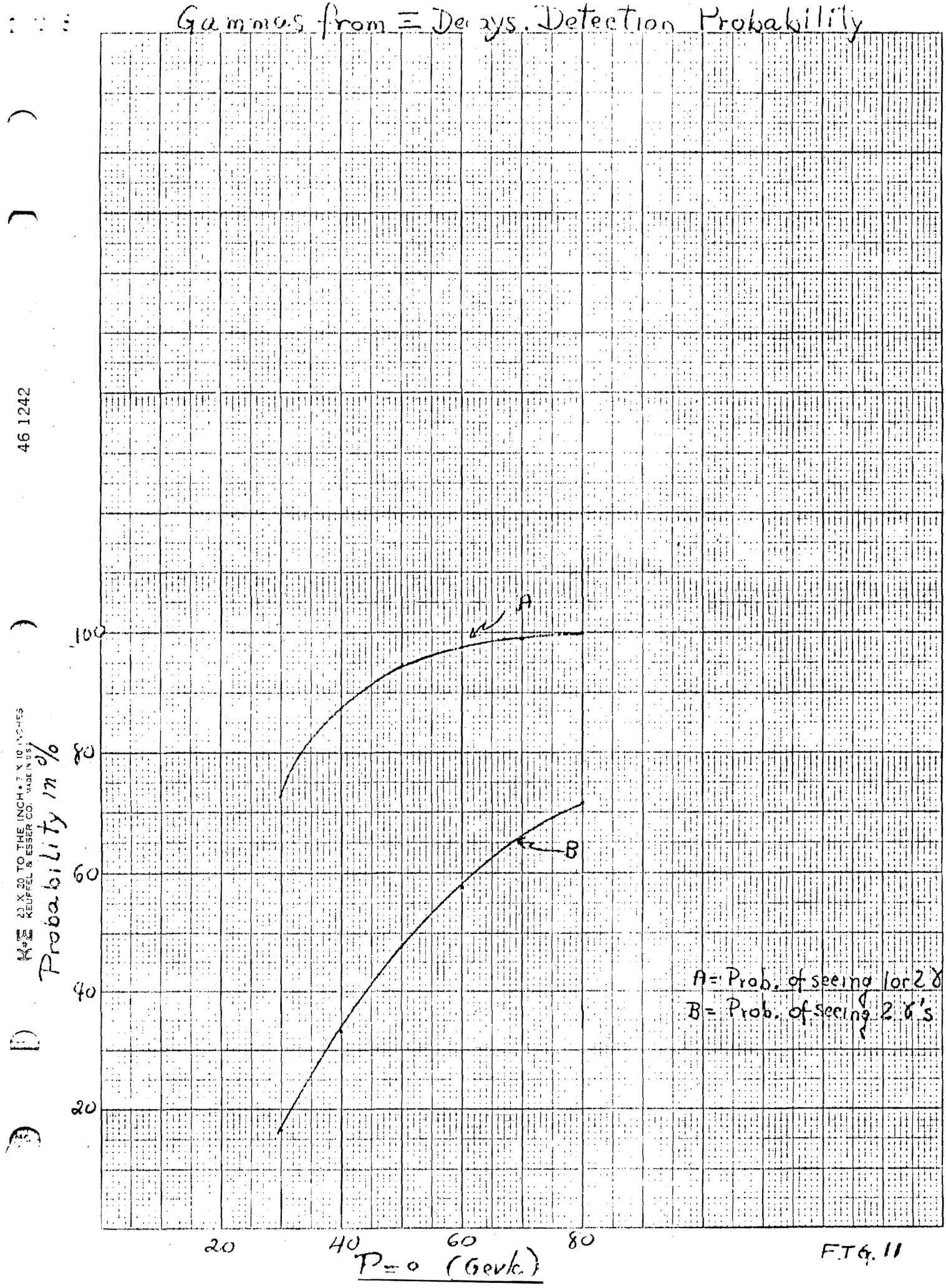
Gammas from Π Decays. Detection Probability
Probability in %
100
80
60
40
20
A
B
A = Prob. of seeing 1 or 2 γ
B = Prob. of seeing 2 γ's
20
40
60
80
P = 0 (Gevk.)
46 1242
K&E 20 X 20 TO THE INCH • 7 X 10 INCHES
KEUFFEL & ESSER CO. MADE IN U.S.A.

FIG. 11

K+E 20 X 20 TO THE INCH • 7 X 10 INCHES KEUFFEL & ESSER CO. MADE IN U.S.A.

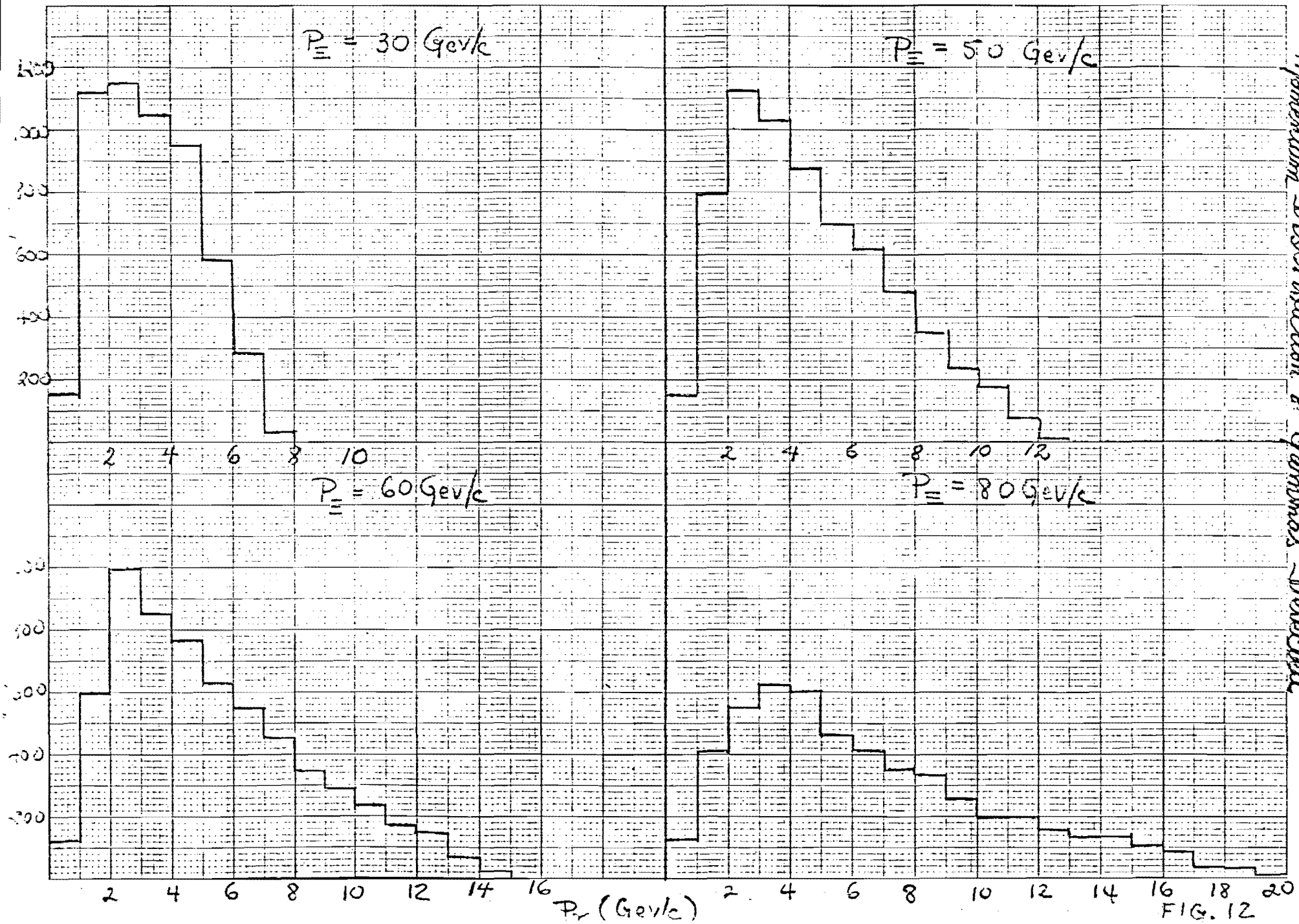

Momentum Distribution of Gammas Detected

FIG. 12

K+E 10 X 10 TO THE CENTIMETER 46 1510
18 X 25 CM. MADE IN U.S.A.
KEUFFEL & ESSER CO.

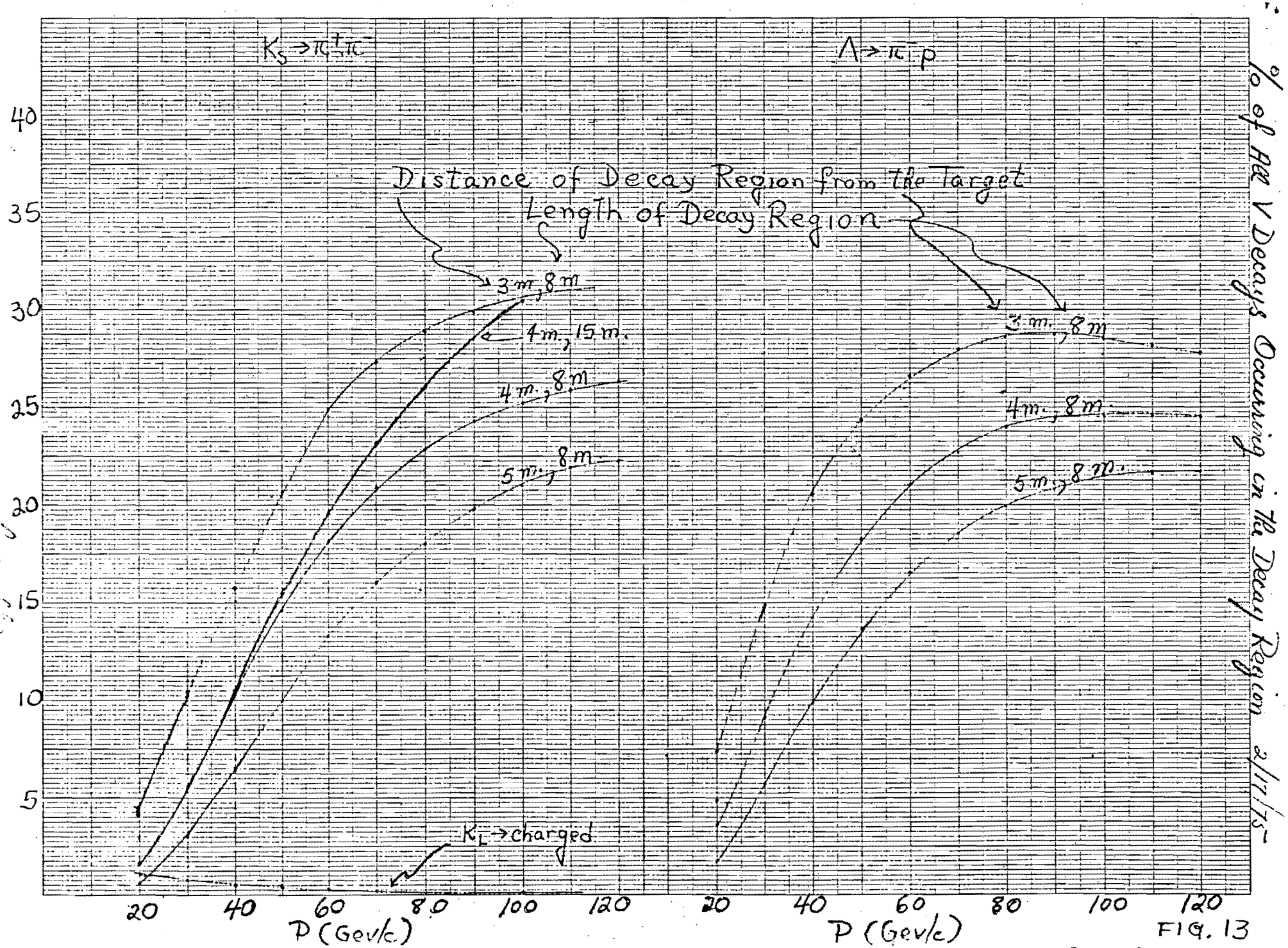

FIG. 13

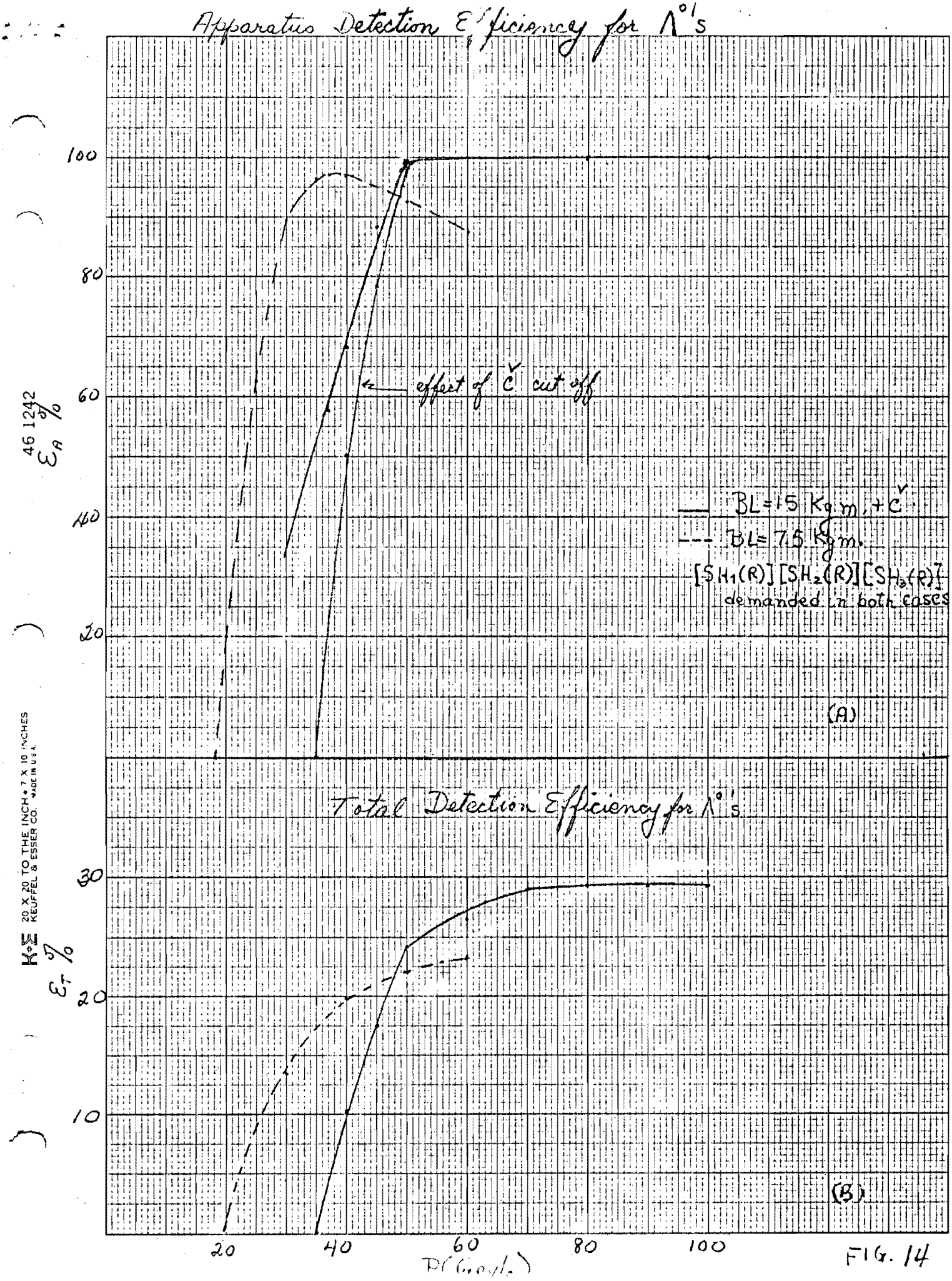
Apparatus Detection Efficiency for Λ°'s
100
80
60
40
20
ε_A %
46 1242
effect of Č cut off
BL=15 Kg m. + Č
BL=7.5 Kg m.
[SH1(R)][SH2(R)][SH3(R)]
demanded in both cases
(A)
Total Detection Efficiency for Λ°'s
30
20
10
ε_T %
(B)
20
40
60
80
100
P(Gev/c)
K+E 20 X 20 TO THE INCH • 7 X 10 INCHES
KEUFFEL & ESSER CO. MADE IN U.S.A.

FIG. 14

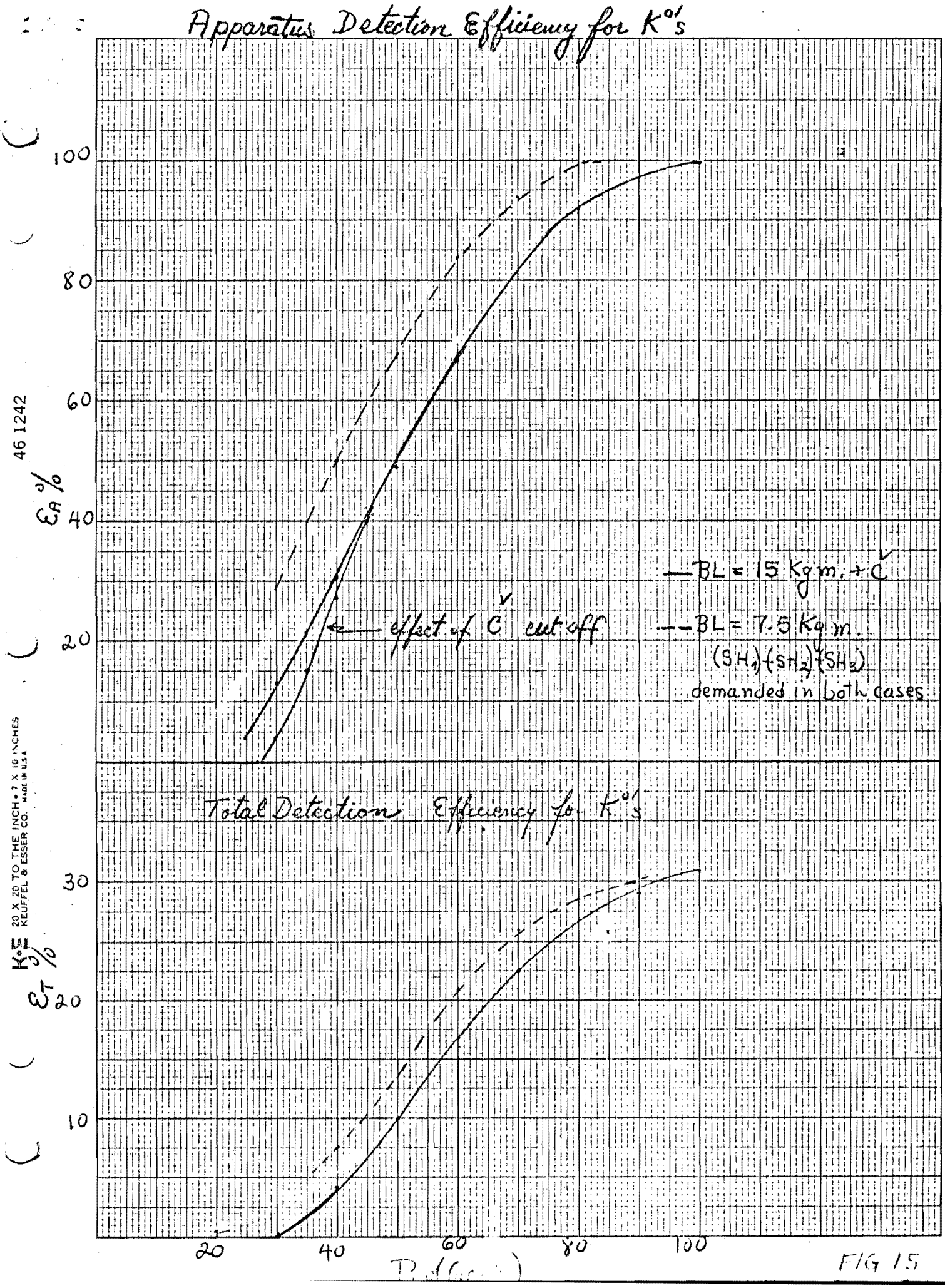
Apparatus Detection Efficiency for K°'s
100
80
60
40
20
ε_A %
— BL = 15 Kg m. + $\check{C}$
effect of $\check{C}$ cut off
-- BL = 7.5 Kg m.
$(SH_1)(SH_2)(SH_3)$
demanded in both cases
Total Detection Efficiency for K°'s
30
20
10
ε_T %
20
40
60
80
100
46 1242
K&E 20 X 20 TO THE INCH • 7 X 10 INCHES
KEUFFEL & ESSER CO. MADE IN U.S.A.

FIG 15

Expected Error Δ Pol. in 400 hours of Data

400 hours = 1.44×10^5 pulses

$$\Delta P = \frac{1}{\alpha}\sqrt{\frac{3}{N}} = \frac{1}{.65}\sqrt{\frac{3}{N}}$$

N = # of Λ^0s observed

α = Λ^0 decay parameter

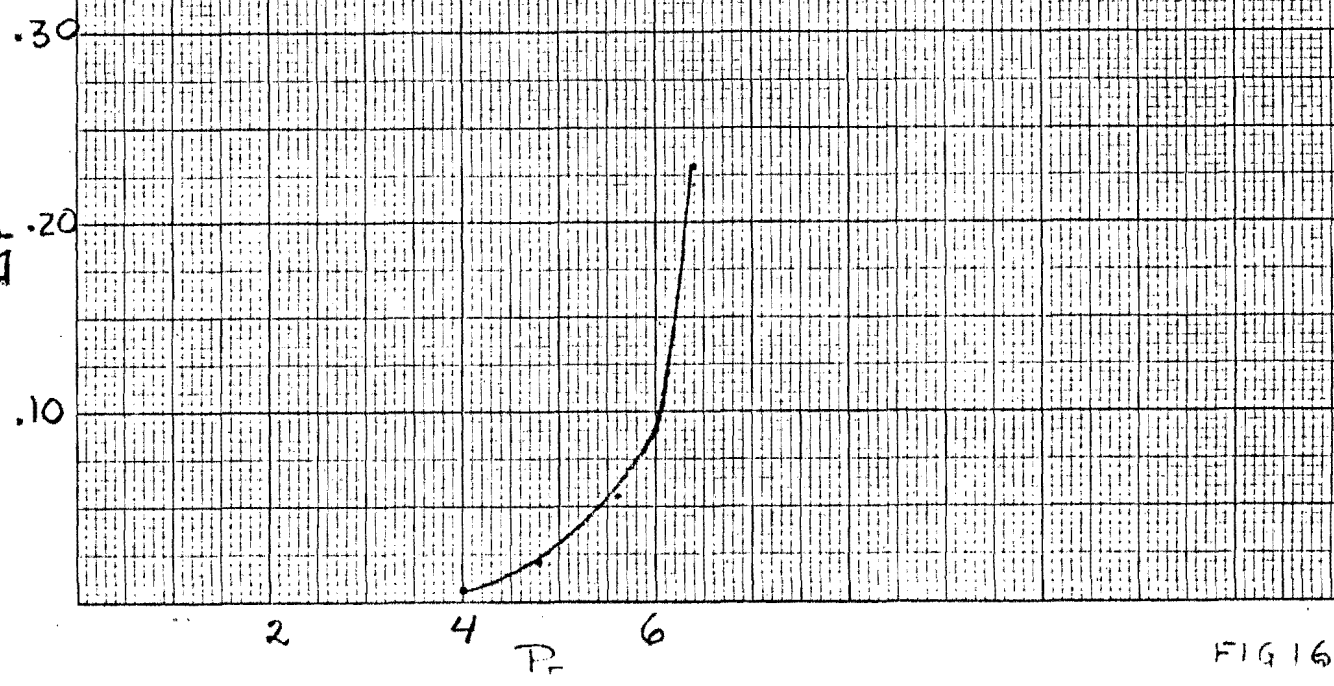

FIG 16

46 1242
K+E 20 X 20 TO THE INCH • 7 X 10 INCHES
KEUFFEL & ESSER CO. MADE IN U.S.A.